

1 **Vegetation interactions with geotechnical properties and erodibility of salt marsh sediments**

2 Evans, B.R.; Brooks, H.; Chirol, C.; Kirkham, M.K.; Möller, I.; Royse, K.; Spencer, K.; Spencer, T.

3

4 **Abstract:**

5 Salt marshes provide diverse ecosystem services including coastal protection, habitat provision and
6 carbon sequestration. The loss of salt marshes is a global scale phenomenon, of great socio-economic
7 concern due to the substantial benefits that they provide. However, the causes of spatial variability in
8 marsh loss rates are inadequately understood for the purposes of predicting future ecosystem
9 distributions and functions under global environmental change. This study investigated the
10 relationship between the presence of different saltmarsh plants and the mechanical properties of the
11 underlying substrate that relate to its vulnerability to erosion. Relationships between three halophytes
12 (*Puccinellia spp.*, *Spartina spp.* and *Salicornia spp.*) and sediment stability were assessed and
13 compared to unvegetated substrates using *in-situ* and laboratory tests of substrate geotechnical
14 properties and sediment characteristics. Sampling was conducted at two UK sites with contrasting
15 sedimentology, one sand-dominated and one clay-rich. Sediment samples, collected simultaneously
16 with measurements of shear strength, were analysed for moisture content, particle size and organic,
17 carbonate and mineral compositions. These data were then used to explore the contribution of plant
18 type, alongside the sedimentological parameters, to measured shear strength.

19 Shear strength of the sediment varied between and, to a lesser extent, within sites, with the four cover
20 types having a similar effect on shear strength within sites relative to each other. Sediments covered
21 by *Puccinellia spp* exhibit the highest shear strength, while bare sediments exhibit the lowest. The
22 effect of vegetation type on shear strength was greater in the coarser sediments of Warton Sands.
23 Surface cover type made a significant contribution to exploratory statistical models developed for the
24 prediction of sediment shear strength. The findings support existing recognition that vegetation can
25 enhance sediment shear strengths but extend the insight to reveal differences in this effect that show
26 generality between sedimentological settings. Further, the combination of methods provides insight
27 into the fundamental mechanics by which various measures of sediment stability may be affected by
28 different surface cover types. Cohesion appears to be a more appropriate descriptor of sediment
29 erodibility than shear strength or friction angle and is most greatly enhanced by the presence of a fine,
30 fibrous root system such as that of *Puccinellia*. A more detailed understanding of the multi-scale
31 mechanisms by which plants confer strength to substrates is needed to better anticipate their impact
32 on sediment erodibility, and therefore salt marsh vulnerability.

33 **Introduction:**

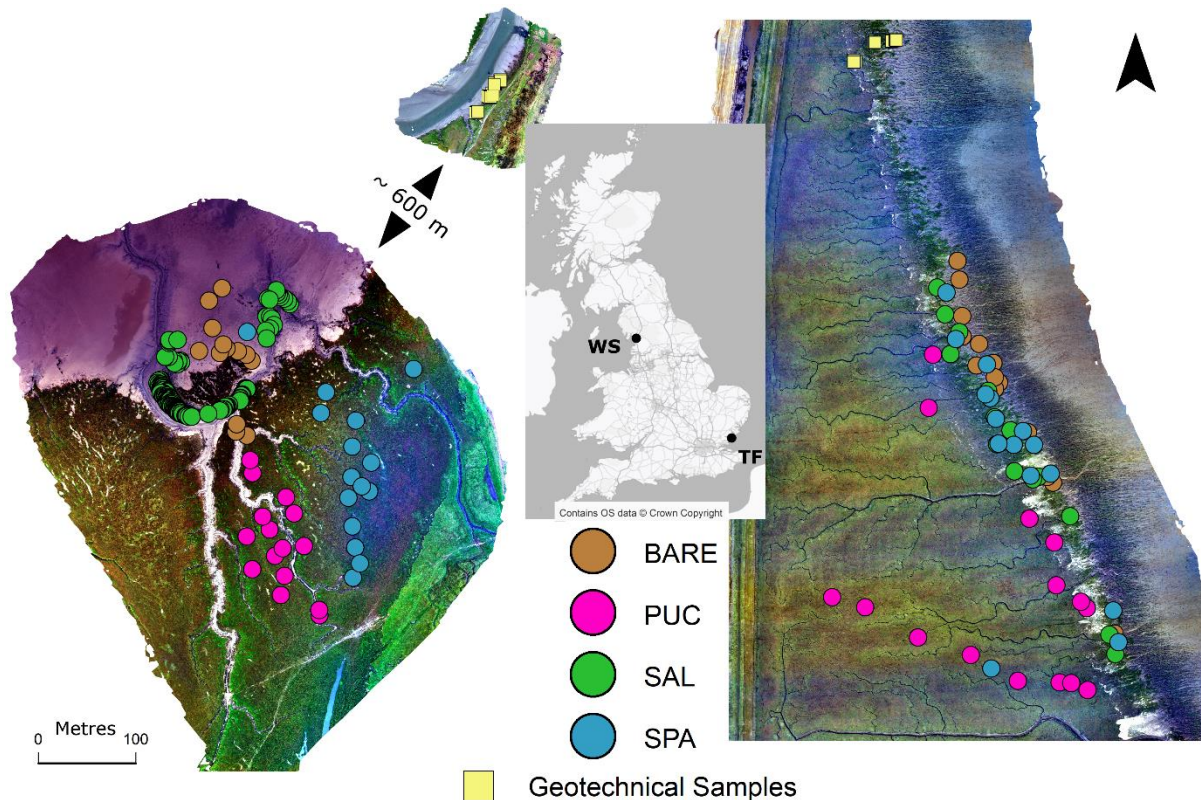
34 Salt marshes are highly valuable coastal biogeomorphic systems with global distributions on both
35 temperate (McOwen et al., 2017) and tropical (Friess et al., 2012) coasts. They provide functions
36 which include coastal protection (Fagherazzi, 2014, Möller et al., 2014) and carbon sequestration
37 (Chmura, 2013) The long-term persistence of these landforms and their associated biota is of
38 paramount importance in the context of global environmental change, yet they are commonly
39 thought to be highly vulnerable to factors such as sea level rise and increased wave exposure
40 (Crosby et al., 2016; Leonardi et al., 2016). An important, but still poorly understood, factor in
41 determining marsh persistence, particularly in terms of lateral erosion processes occurring at their
42 seaward margins, is the stability of the sediments in response to hydrodynamic forcing. This is widely
43 recognised as fundamental for the prediction of morphological change (Brooks et al., 2021). The
44 geotechnical attributes of a substrate (the parameters describing the ways in which it deforms and

45 fails when force is applied) are important for understanding its response to hydrodynamic forcing.
46 These attributes are, however, difficult to measure and observe across the large areas required to
47 capture the spatial heterogeneity in factors controlling marsh margin erosion rates. There is also
48 increasing recognition that salt marsh vegetation plays an important role in determining substrate
49 stability (Bernik et al., 2018; Chen et al., 2019; Ford et al., 2016), with the influence of vegetation
50 being stronger in coarser sediments (De Battisti et al., 2019; Lo et al., 2017a). Grazing or mowing
51 regimes that favour the establishment of plants with high root density have been shown to reduce
52 the erodibility of marsh sediment under flume conditions (Marin-Diaz et al., 2021) Wang et al. (2017)
53 also found belowground biomass and vegetation species to affect sediment erodibility in a flume
54 context. Many of these studies use flumes or cohesive strength meters to observe the erosion
55 resulting from particular flows of water. These observations, however, don't elucidate the processes
56 by which the vegetation confers strength to the substrate and don't furnish estimates of shear
57 strength and are thus difficult to incorporate into numerical simulation frameworks. This study
58 therefore applies a range of geotechnical measurement approaches to different vegetation species
59 and sediment types to provide mechanistic insight to the ways in which different plant species
60 modify the properties of sediments. This study investigates whether different species of saltmarsh
61 plant, exhibiting different growth forms and root structures (Chirol et al., 2021a), produce different
62 controls on substrate geotechnical properties and sediment erodibility. If this were to be the case,
63 then relatively simple vegetation survey methods, such as mapping from aerial or satellite imagery,
64 might be used to characterise a component of the spatial variability in substrate properties. Such an
65 approach would support numerical simulation, and site-based predictions, of system vulnerability to
66 hydrodynamic/meteorological forcing. In this study, laboratory and field geotechnical measurements
67 are applied to substrates from two types of substrate, each vegetated by three different species.
68 Comparisons are also made to the attributes of unvegetated surfaces. In order to explore the
69 mechanisms by which these differences may relate to the stability of larger landform units,
70 differences in geotechnical response by surface cover type are explored, and interpreted in the
71 context of the differing three-dimensional root network structures of the species involved (Chirol et
72 al., 2021a). The way in which spatio-temporal vegetation distributions may affect site-scale erosion
73 trajectories is illustrated through a conceptual model that could form the basis for numerical
74 simulation in future work.

75 [Study locations:](#)

76 Sites were selected from contrasting biosedimentary regimes representative of the approximate end-
77 member conditions for the range of sediments observed within salt marsh systems in the UK. Warton
78 Sands (WS), in Northwest England, sits within the wider Morecambe Bay system. It is macro-tidal
79 environment with a mean spring tidal range of 8.49m at Heysham, 13 km from the site (National Tidal
80 and Sea Level Facility, 2021). The WS sediments are coarse with a high proportion of sand. Tillingham
81 Farm (TF) is an open-coast marsh located on the macro-tidal Dengie Peninsula, Essex, in the Southeast
82 of England. Mean spring tidal range at Sheerness, 30 km from the site, is 5.21m (National Tidal and
83 Sea Level Facility, 2021) and the sediments are finer, containing a higher proportion of clay and silt
84 than WS (see results for sedimentological descriptions). Vegetation communities show differences at
85 the scale of each site, but both locations contain monospecific areas of the three halophytes
86 investigated in this study, allowing a comparison to be drawn at the patch scale. Figure 1 shows the
87 study locations and sampling distributions.

88

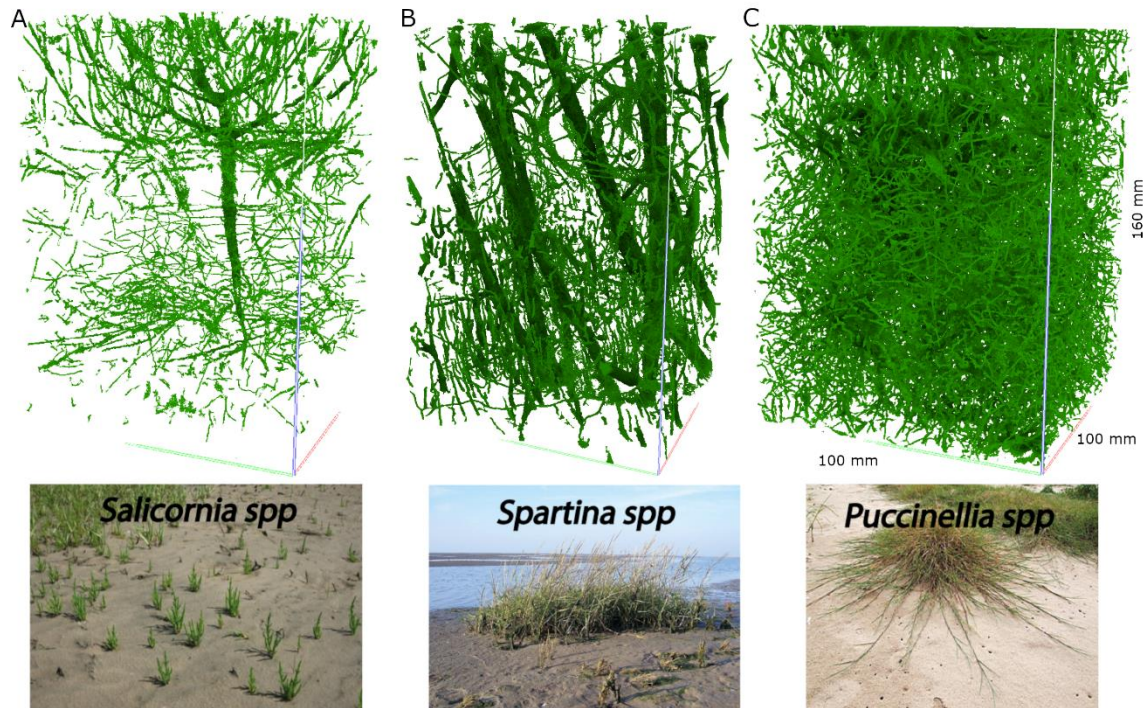


89

90 Figure 1 - Study locations at Warton Sands (WS, left) and Tillingham Farm (TF, right) showing sampling locations (circles) for
 91 shear vane and associated sedimentology for the four cover types investigated, and geotechnical laboratory sample
 92 locations (squares). UAV orthomosaics by B Evans, left to right: 22/09/2019, 18/01/2019, 08/08/2019.

93 **Methods:**

94 Two sampling campaigns were conducted, one in Winter 2018-2019 and one in Summer 2019; in the
 95 winter campaign undisturbed cores were extracted for laboratory testing by shear box, tor vane and
 96 triaxial tests (square symbols, Figure 1 - Study locations at Warton Sands (WS, left) and Tillingham
 97 Farm (TF, right) showing sampling locations (circles) for shear vane and associated sedimentology for
 98 the four cover types investigated, and geotechnical laboratory sample locations (squares). UAV
 99 orthomosaics by B Evans, left to right: 22/09/2019, 18/01/2019, 08/08/2019. Figure 1). In the
 100 summer campaign, *in-situ* shear vane measurements were taken alongside sediment sampling and
 101 ground survey to characterise vegetation distributions (circles, Figure 1). Three plant species were
 102 investigated. These were *Puccinellia spp.* (PUC), *Spartina spp.* (SPA), and *Salicornia spp.* (SAL).
 103 Unvegetated sediments, lacking vascular plant cover, were sampled as a control (BARE) to provide
 104 four surface cover types at each site. The plant species were selected because they have contrasting
 105 root morphologies. *Salicornia* has a sparse tap root structure, *Spartina* has a denser, thicker tap root,
 106 while *Puccinellia* has a dense network of fine, fibrous roots. These differences are discussed further
 107 in (Chiról et al., 2021a), where they are hypothesised to influence sediment characteristics in
 108 contrasting ways. Photographs of each species and representations of the undisturbed root 3-
 109 dimensional network maps derived from micro-CT scans of cores are presented in Figure 2 to
 110 illustrate the morphological contrasts.



111

112 *Figure 2 - photographs (bottom) and undisturbed root network segmentations (top) for the three species investigated,*
 113 *Salicornia (A), Spartina (B) and Puccinellia (C). Adapted from Chirolet al.(2021a), figures 2 and 3.*

114 The winter campaign was conducted on 12th-13th January at TF and 18th-19th January at WS. The
 115 summer campaign was conducted at TF on 8th-9th August and WS on the 21st-22nd September. We
 116 assume that the effects of the root networks on geotechnical properties follows the same relative
 117 relationship in winter and summer, even if the magnitude of any effect may vary, since the root
 118 networks of all species investigated persist inter-annually despite seasonal dieback of above-ground
 119 elements. Our analysis takes into account that antecedent conditions may have resulted in
 120 differences in moisture between sites (see below).

121 In Winter, undisturbed cores of 150 mm diameter and 150 mm depth were extracted for shear box
 122 analysis following the careful procedure described in Chirolet et al. (2021b). The same procedure was
 123 used to extract 100 mm diameter, 200 mm long cores for triaxial testing (BS1377: Part 8:1990
 124 Method 7). Three replicate cores were extracted from monospecific patches of each plant type (PUC,
 125 SPA, SAL) and unvegetated sediment (BARE). Cores were packaged in insulated, padded containers
 126 and returned to the laboratory where they were cold stored at 5°C while awaiting analysis. Samples
 127 were analysed sequentially, such that storage periods for some were substantially longer than for
 128 others as a consequence of the time required for analysing each sample. This may affect the results
 129 obtained to some extent (Tolhurst et al., 2000).

130 In summer, measurements and samples were taken within fifteen 1m² quadrats for each plant type
 131 where the vegetation cover was monospecific or very heavily dominated by the relevant (visual
 132 estimate of 95-100% cover). The exception was SAL at Warton, where no patches larger than 1m²
 133 were found. Shear vane tests were therefore conducted immediately adjacent to the relatively
 134 sparsely distributed individuals.

135 **Shear box tests:**

136 Following μ CT scanning, the shear strength of a subset of the cores was tested using a Wykeham
 137 Farrance Model No. 25402 shear box apparatus at the British Geological Survey, Keyworth, UK.

138 Shear box testing is time-consuming so it was not possible to test all surface cover/sediment type
139 combinations for which samples were acquired. WS BARE and TF BARE were tested to isolate the
140 differences in shear strength arising from the differing sediment types of the sites without
141 vegetation influences. TF PUC and TF SPA were also tested as these have substantially different root
142 network morphologies (Chiril, et al., 2021a) which might be expected to influence substrate shear
143 characteristics. Cores were removed from their plastic cases and sub-sampled by the same careful
144 trimming method as used for field collection. Three 60mm by 60mm by 20mm shear box samples
145 were extracted at different depths along the vertical axis of each core. These three sub-samples
146 were then tested using the standard shear box procedure to BS1377 (BSI, 1990, pp48). A normal
147 (vertical) stress was applied to each subsample (20, 40 or 80 kPa) and the sample sheared
148 horizontally while the imposed stress and resulting strain were monitored. Estimates of cohesion (c)
149 and friction angle (ϕ) were calculated by fitting a least-squares regression line through the peak
150 stress values of the three resulting stress-strain curves. Thus, the shearing of three sub-samples
151 constitutes a single shear box test. Cohesion is represented by the intercept of the regression line
152 while friction angle is the inverse tan of the slope coefficient. Strain rates were maintained at 0.05
153 mm min⁻¹, low enough to allow pore pressures to equalise during deformation, based on initial
154 consolidation characteristics. The shear box test was, therefore, considered to be a 'drained' test. As
155 a result of COVID-19 restrictions, it was not possible to complete all planned shear box tests and only
156 two replicates were achieved for WS BARE and TF BARE compared to three replicates for TF PUC and
157 TF SPA. Much of the existing literature, however, does not attempt any replication of shear box tests
158 in order to infer geotechnical attributes (e.g. Ali & Osman, 2008; Mouazen, 2002; Wang et al., 2013;
159 Zhou et al., 2019).

160 Figure 3 shows vertical photographs of the 60 mm square shear box cutting shoe that was used with
161 sediments from the four surface cover types tested. Contrasting granulometry, pore and root
162 structures are clearly visible.



163

164 *Figure 3 – Vertical photographs of Shear box samples from four surface cover types. Top left TF BARE,*
165 *top right TF PUC, bottom left TF SPA, bottom right WS BARE. Samples are 60x60 mm and are sheared*
166 *along the plane depicted.*

167

168 **Torvane shear testing (laboratory):**

169 During sub-sampling for the shear box tests, the cores were trimmed to a 110mm square column. A
170 Gilson HM504-A torvane was used at two depths (centred at 50 and 100mm) on each side of this
171 column to provide eight measurements per core which were then averaged. Further trimming was
172 then conducted for the shear box tests. The torvane is a spring-loaded torque meter with short
173 vanes on a circular disc. Vanes are inserted into the soil by about 5mm until the disc sits flush with
174 the sediment surface. The handle is twisted until the sediment shears and the vanes spin. The
175 maximum torque thus applied is read from a dial and converted to shear strength by applying a
176 calibration factor (Jafari et al., 2019).

177 **Triaxial tests:**

178 Triaxial tests were conducted on undisturbed cores of 102mm diameter and approximately 200mm
179 height using a GDS Labs triaxial tester to the BS1377 Part 8 (1990) standard. Tests were made on one
180 sample from each site/surface cover type combination, resulting in eight tests being conducted.
181 Constraining pressures of 5, 10 and 20 kPa were used to assess behaviour of these sediments under
182 realistic ranges of hydrostatic forcing. For example, 5 kPa is equivalent to the loading from a 0.51 m
183 column of pure water, while 20 kPa equates to 2.0 m. Thus we simulated approximate
184 hydrostatic/hydrodynamic loadings that may be experienced by NW European marsh sediments
185 under both normal and storm surge conditions. Wet bulk density was calculated for each sample
186 prior to testing.

187 **Shear vane (field):**

188 Sediment shear strength was measured in the field using two H-60 vane testers. These are spring-
189 loaded torque meters akin to the torvane except that their vanes are radial and protrude from a
190 shaft, allowing for measurement within the sediment rather than at its surface. Vanes were inserted
191 to a depth of 7.5 cm in order to engage with the active root layer of the vegetation. Shear strength
192 was measured at 15 monospecific 1 m by 1 m quadrats per surface cover type (Figure 1) with ten
193 randomly located measurements per quadrat. In the case of WS SAL, shear vane measurements
194 were conducted immediately adjacent to 150 individual plants. The shear vane data have been
195 previously described (Chiról et al., 2021a) but this study relates these observations to sedimentology
196 directly associated with the shear vane sampling locations rather than proximal sediment cores.

197 **Sedimentology:**

198 Sediment samples were taken within the top 7.5cm depth at each quadrat. In the case of WS SAL,
199 sediment samples were taken at every tenth sampling point at which the shear vane was used.
200 samples subsampled to provide three replicates for laser particle size analysis using a Malvern
201 Mastersizer and providing a particle size distribution (PSD), and for composition by loss-on-ignition.
202 Loss-on-ignition was conducted at incrementally increasing temperatures of 105°C, 400°C, 480°C and
203 950°C, with samples being heated for six hours per temperature before weighing. These furnished
204 estimates of percentage composition of water, carbohydrates, total organics and calcium carbonate
205 respectively.

206 **Statistical analyses:**

207 Differences in sediment shear strength and characteristics between sites and surface cover types
208 were tested in Matlab software using the Kruskal-Wallis test followed by multiple-comparison
209 compensation (Dunn-Sidak). To avoid inflated type 1 error rates related to pseudoreplication in the
210 case of the shear vane and torvane, the mean of measurements from each quadrat or core
211 respectively was used to represent that replicate in the Kruskal-Wallis tests. Since sample sizes were
212 small and it was not possible to test for homoscedasticity between treatments, we formulated our
213 Kruskal-Wallis tests in terms of stochastic dominance rather than differences in medians, whereby
214 the existence of stochastic dominance implies that samples drawn from one treatment are likely to
215 be higher than samples drawn from a contrasting treatment. Correlations between measurements
216 acquired by different tests were used to explore how the data provided by different methods relate
217 to each other. Exploratory modelling to investigate how different parameters affect shear strength,
218 as measured by the shear vane, was conducted in R (R Core Team, 2013) using boosted regression
219 trees (BRTs) and the 'gbm' package (Elith et al., 2008). The sedimentological parameters of median
220 grain size (d50), proportion below 63µm (Below63), Kurtosis of PSD, Skewness of PSD, percentage
221 total organics (Organics), percentage water (Moisture), and percentage Calcium Carbonate (CaCO₃)
222 alongside surface cover type (CoverType) were used as predictors for shear strength (dependent

223 variable). Given that antecedent conditions, rather than vegetation or sediment factors, are likely to
224 account for differences in moisture between sites, the analysis reported here focussed on within-site
225 controls. The boosting process introduces a degree of stochasticity to model results. Elith et al.
226 (2008) argue that this effect is subtle and unlikely to affect model interpretation so results from a
227 single training of the model are reported here. Elith et al. (2008) recommend that models should be
228 fitted using between 10^3 and 10^4 trees to optimise generality and control overfitting. This is
229 achieved by tuning the hyperparameters of tree complexity (controlling the number of branches
230 within each tree) and the learning rate (which controls the contribution of each tree to the ensemble
231 result). A tree complexity of 6 and a learning rate of 0.001 were used, typically producing models
232 based on between 2000 and 4000 trees. All predictors were provided to the algorithm to develop
233 benchmark models. The 'gbm.simplify' function was then used to drop uninformative predictors and
234 select a parsimonious final model that optimised performance (Miller, 2002). For exploratory
235 purposes, the model performance was evaluated based on the training correlation and using 10-fold
236 cross-validation.

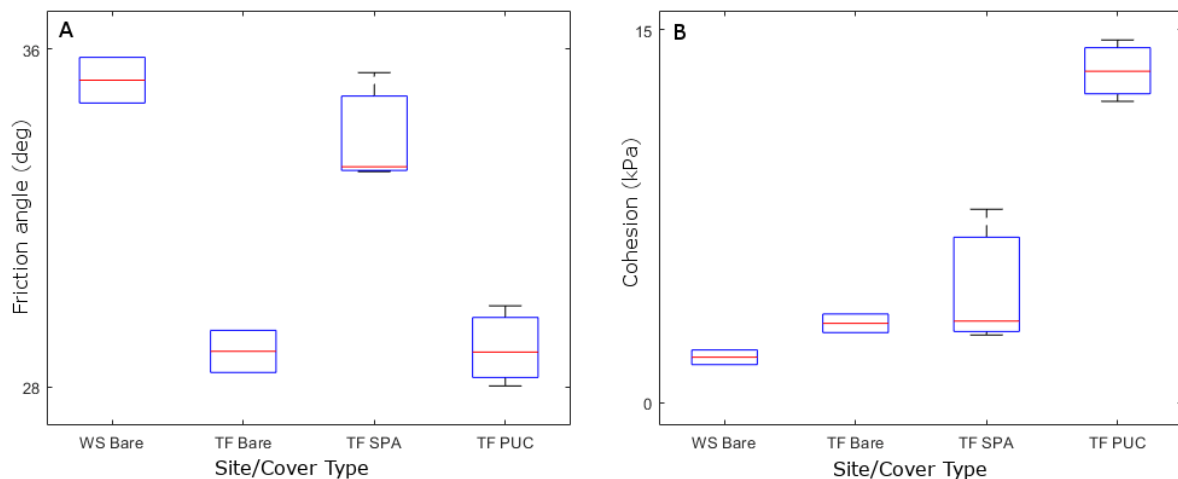
237

238 Results:

239 Shear box

240 The shear box test produced estimates of cohesion and friction angle (Figure 4). A Kruskal-Wallis test
241 for stochastic dominance between cover types returned p-values of 0.066 for friction angle and
242 0.054 for cohesion. Subsequent multiple comparison analysis showed stochastic dominance in terms
243 of cohesion for WS BARE being lower than TF PUC.

244



245

246 *Figure 4 - Boxplots of friction angle (A) and cohesion (B) derived from shear box tests. WS BARE and TF BARE n=2, TF SPA*
247 *and TF PUC n=3*

248 Peak shear strength at 20 kPa normal stress correlated strongly with moisture content of the sample
249 prior to testing, with a Pearson's R of 0.73, while at 40 kPa and 80 kPa this correlation was weak
250 (R=0.18 and 0.08 respectively, n=10). Friction angle and cohesion were negatively correlated (R = -
251 0.66, n=10).

252

253 **Torvane:**

254 Torvane measurements taken while preparing shear box samples produced mean shear strength
255 measurements for TF BARE of 12.27 kPa, TF PUC of 13.77 kPa, TF SPA of 13.24 kPa and WS BARE of
256 8.91 kPa. Populations were analysed for stochastic dominance of shear strengths between surface
257 cover types using a Kruskal-Wallis test followed by multiple comparison. WS BARE shear strength
258 was significantly lower than all three TF cover types ($p < 0.01$). No significant differences were found
259 between the TF cover types themselves ($p > 0.59$ in all cases).

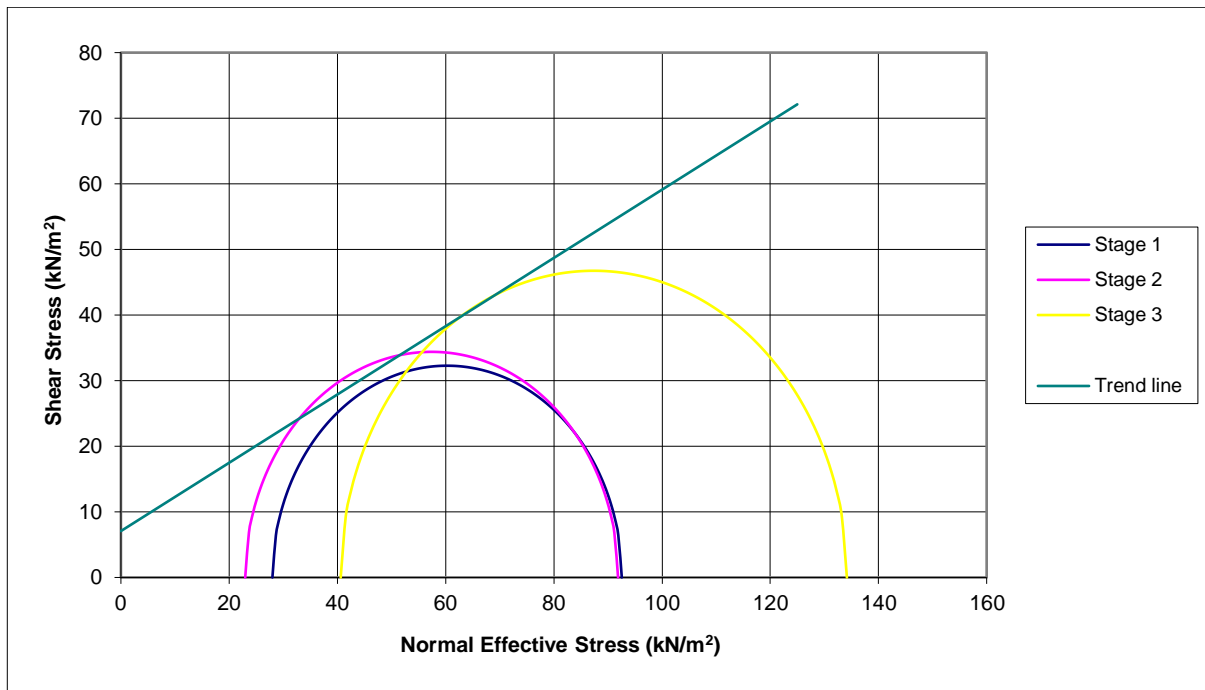
260 Torvane shear strengths correlated moderately with shear box peak shear strengths at 20 kPa
261 normal stress, but not at 40 kPa or 80 kPa with Pearson's R of 0.58, 0.09 and 0.10 respectively.
262 Moderate positive correlation was found between torvane shear strength and shear box cohesion (R
263 = 0.50) while a moderate negative correlation was found for friction angle ($R = -0.44$). There was a
264 moderate positive correlation between torvane shear strength and moisture ($R=0.47$), driven largely
265 by inter-site differences in moisture content.

266

267 **Triaxial tests:**

268 The narrow range of confining pressures that were adopted to test behaviour under realistic
269 hydrostatic/dynamic pressures for surface sediments at the two sites resulted in significant overlap
270 between Mohr circles calculated at each test stage. As a consequence, it was not possible to fit
271 robust trendlines through these circles and six of the eight tests returned negative, or null, estimates
272 of cohesion. Negative values of cohesion are not physically meaningful so cannot be interpreted. The
273 tests that returned positive cohesion estimates were WS PUC and WS SPA, returning cohesion
274 estimates of 7.08 kPa and 3.16 kPa and friction angles of 27.49° and 31.3° respectively. These values
275 are broadly comparable to those acquired from the shear box tests, although WS PUC and WS SAL
276 were not assessed in the shear box. Figure 5 shows the resulting Mohr circles and trend line
277 for the WS PUC test. As is evident, a large amount of overlap still occurs in this sample. Some of this
278 overlap arises from the fact that the equipment used was unable to maintain the effective stress to
279 the required degree of precision. Some overlap may arise from incomplete consolidation which is
280 typically negligible when testing across a wider range of effective stresses.

281



282

283 *Figure 5 - Mohr circles from triaxial shear test on WS PUC, with cohesion (y-intercept) of 7.08 kPa and*
 284 *friction angle (arc-tangent of slope) of 27.49°, with substantial overlap between Stage 1 and Stage 2.*

285 Wet bulk densities for all combinations of site and cover type are shown in table XX

286 *Table 1 - wet bulk density for eight combinations of site and surface cover type derived from triaxial test samples*

Site/Cover Type combination	Wet bulk density (kg m ⁻³)
TF_BARE	1590.79
TF_PUC	1422.68
TF_SAL	1520.04
TF_SPA	1272.32
WS_BARE	1905.44
WS_PUC	1877.99
WS_SAL	1851.73
WS_SPA	1731.29

287

288

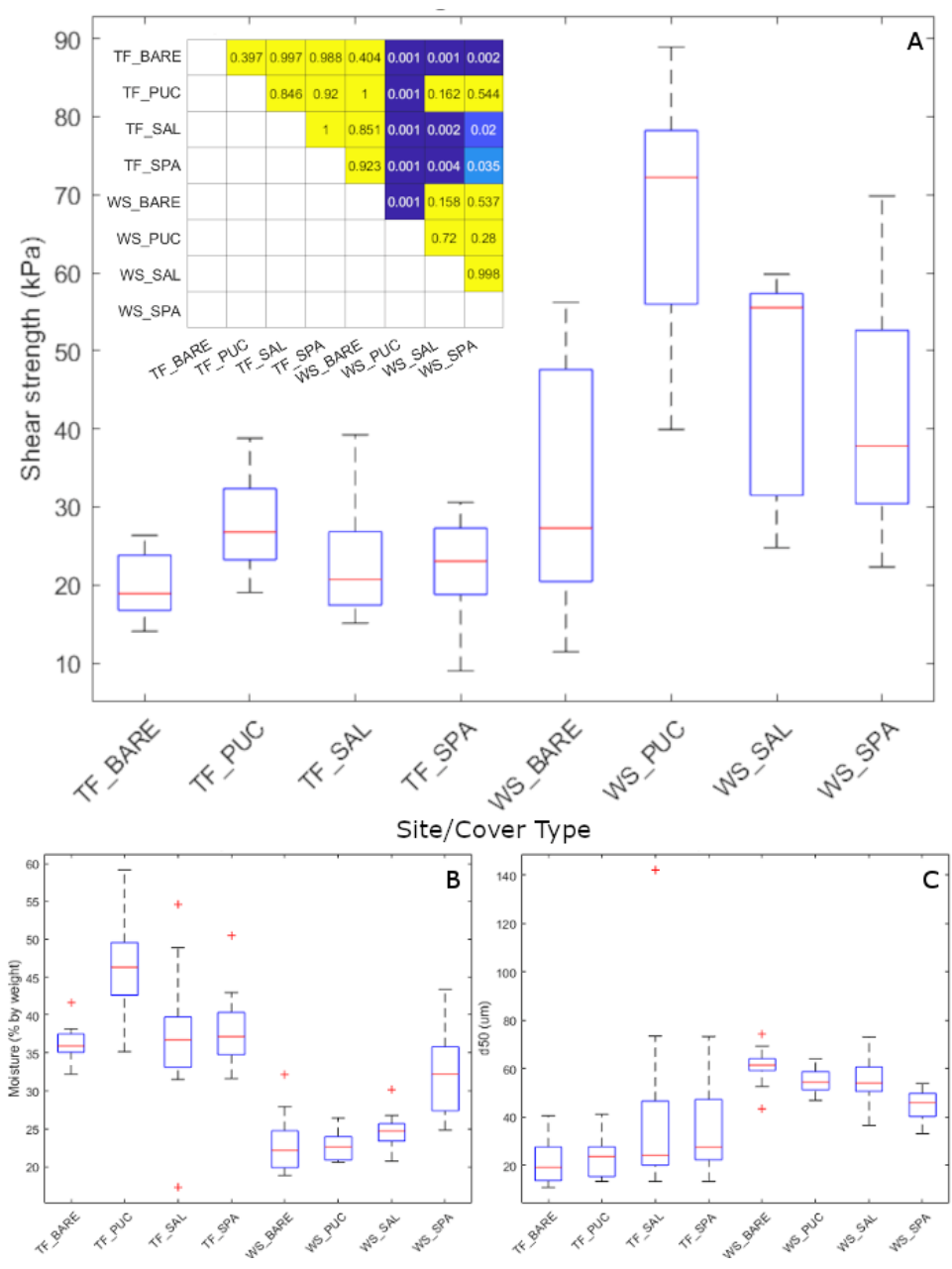
289

290 **Variability in sediment parameters measured in the field**

291 Shear strength, measured in the field by the shear vane, showed differences between treatments
 292 (Kruskal-Wallis $p < 0.001$). post-hoc comparisons showed no differences between cover types within
 293 sites, with the exception of WS PUC, which contrasted with WS BARE. Widespread differences were
 294 observed between sites with the exception of TF PUC, which was not separable from WS SAL and WS
 295 SPA. Within sites the pattern of PUC being strongest, SPA and SAL being very similar and BARE being
 296 weakest is consistent between sites, even though the sample populations are not statistically
 297 separable at the level of replication available. The moisture contents and median grain sizes of the
 298 sediments showed similar inter-site differences, but not within-site variability between surface cover
 299 types, (Figure 6, panels B and C). Kruskal-Wallis tests returned p -values < 0.001 for both parameters,

300 suggesting that stochastic dominance exists between treatment groups. Subsequent multiple
 301 comparisons showed widespread contrasts in both moisture and d_{50} between sites, but no
 302 differences between plant surface cover types within sites, with the exception of separability
 303 between WS SPA and both WS BARE and WS PUC (Table 2). WS SPA, having the finest and wettest
 304 sediments found at WS, was not separable from the vegetated TF surface cover types in terms of d_{50} ,
 305 nor was its moisture content separable from TF cover types with the exception of TF PUC, which was
 306 the driest TF cover type.

307
 308



309
 310 *Figure 6 – Panel A - Shear strengths measured in the field using H-60 vane tester. Inset matrix shows*
 311 *p-values of post-hoc multiple comparisons following Kruskal-Wallis test for differences between*
 312 *means (blue = significantly different at $p < 0.05$). Panel B – moisture contents. Panel C – median grain*
 313 *size (d_{50}).*

314

315 Variance in shear strength was greater for all cover types at WS than TF. This is in contrast to the
316 variance in moisture content and d_{50} , which was typically smaller at WS than at TF, although WS SPA
317 exhibited greater variance than the other WS cover types, and WS BARE showed greater variance
318 than its TF counterpart. The relatively high variance in moisture for WS SPA did not appear to
319 translate into greater variance in shear strength for this cover type than for the other WS
320 treatments. This may imply that the variability in shear strength at WS is primarily responsive to
321 factors other than the moisture or d_{50} measured here.

322 *Table 2 - Results of Kruskal-Wallis and multiple comparison for differences between moisture and d_{50}*
323 *across eight sample conditions. $n=15$ per condition. Significant ($p < 0.05$) differences denoted by 'M'*
324 *for moisture (upper right) and 'D' for d_{50} (lower left)*

	TF BARE	TF PUC	TF SAL	TF SPA	WS BARE	WS PUC	WS SAL	WS SPA
TF BARE					M	M	M	
TF PUC					M	M	M	M
TF SAL					M	M	M	
TF SPA					M	M	M	
WS BARE	D	D	D	D				M
WS PUC	D	D	D	D				M
WS SAL	D	D		D				
WS SPA	D							

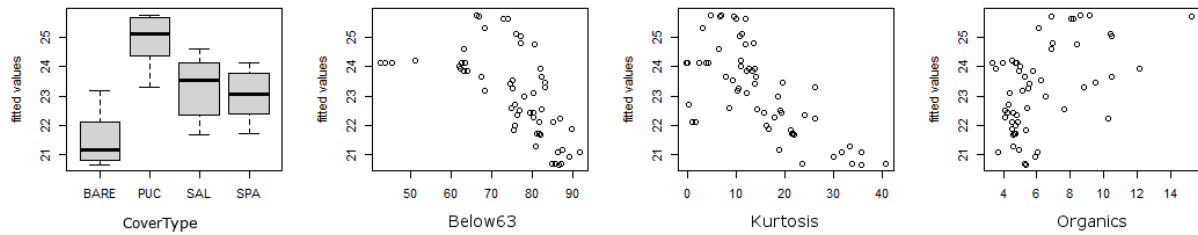
325

326 **Exploratory multivariate modelling:**

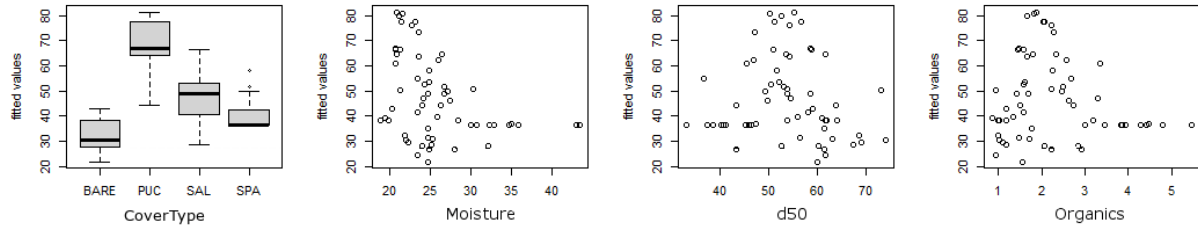
327 At both TF and WS sites, when using the full predictor set, surface cover type contributed most to
328 model fit. The full model at TF produced a training correlation of 0.48 and a cross-validation (CV)
329 correlation of 0.22. Surface cover type contributed 21% to the fit, ahead of the other parameters. At
330 WS, training and CV correlation were considerably higher at 0.90 and 0.69 respectively, with surface
331 cover type contributing 34% to the fit.

332 In the simplified model CoverType, Kurtosis, Below63, and Organics were selected as predictors for
333 the shear strength at TF. Training correlation was 0.48 and CV correlation was 0.28. CoverType and
334 Below63 both contributed 28% to the fit, followed by Kurtosis and Organics, both at 22%. At WS,
335 training correlation was 0.90 and CV correlation was 0.74. CoverType contributed most to the fit at
336 39%, followed by Moisture (27%), d_{50} (20%) and Organics (14%). Fitted values for both models are
337 shown in Figure 7. The improved CV correlations compared to the full models indicate better
338 generality.

TF



WS



339

340 *Figure 7 - Fitted values (kPa) for BRT models predicting shear strength at TF (top) and WS (bottom).*
 341 *Note the contrasting range of shear strength values between sites (vertical axes).*

342 As described previously, the range and variance of the shear strength values obtained were much
 343 higher for WS than TF, probably accounting, in part, for the relatively poor training and CV
 344 correlations at TF. At both sites, the surface cover type exerted a primary influence on the model,
 345 and the relative influences of the different covers were similar at both sites. BARE produces the
 346 lowest shear strengths, while PUC produces the highest, with SAL and SPA resulting in intermediate
 347 shear strengths, with those associated with SAL being somewhat higher. The percentage organic
 348 content of the sediments was selected at both sites, although it was the least informative predictor.
 349 Parameter ranges varied considerably, making direct comparison challenging. Relationships between
 350 shear strength and the percentage of the sediment below 63 μ m and the kurtosis of the particle size
 351 distribution (TF) were moderately well-defined negative associations, while the relationships at WS
 352 with moisture and median grain size were less clear. The low training and CV correlations at TF
 353 means that other factors (not observed here) account for most of the variance in shear strength.
 354 Nevertheless, the coherent patterning of relative effects of cover types when compared to WS, and
 355 the relatively well-defined structure within the Below63 and Kurtosis relationships to shear strength
 356 at TF, provide added confidence that these factors are correctly identified by the model as important
 357 predictors.

358

359 **Discussion**

360 In broad terms the data presented here support the findings of previous studies assessing the effect
 361 of vegetation on salt marsh erodibility in that vegetation is shown to positively affect a number of
 362 parameters often thought to be related to an increase in the stability of marsh sediments (e.g. De
 363 Battisti et al., 2019; Chen et al., 2019; Ford et al., 2016; Lo et al., 2017; Marin-Diaz et al., 2021; H.
 364 Wang et al., 2017). In contrast to many of these studies which have measured sediment erodibility
 365 using hydrodynamic exposure, this study measured sediment geotechnical properties including
 366 shear strength, cohesion and friction angle directly using a variety of methods. Nevertheless, some
 367 commonality in findings emerges, principally that vegetation and sedimentology combine to control
 368 shear strength and erodibility of sediment. It is clear, however, that establishing a general function
 369 to translate between geotechnical attributes and erodibility remains challenging. For example, the
 370 sandier WS sediments studied here produce higher shear strengths and friction angles than their TF

371 counterparts yet are more erodible. The between-site contrast is probably driven by WS having
372 coarser sediments and lower sodium absorption ratio than TF (Chiról et al., 2021a; Grabowski et al.,
373 2011). Meanwhile, within-site increases in shear strength that are observed in vegetated compared
374 to bare sediments can be expected, from the existing literature, to translate into reduced erodibility.
375 Therefore, depending on context, either a positive or negative relationship between shear strength
376 and erodibility is possible, and the sign of this relationship will depend on the mechanism by which
377 shear strength is increased. The torvane measurements, by contrast, showed the bare WS sediment
378 to have significantly lower shear strength than the three TF cover types, including bare ground. This
379 suggests that the shear vane and the tor vane measure different components of the sediment
380 strength, with the relationships found between the torvane measurements and the shear box
381 cohesion and friction angle estimates suggesting that the torvane is more sensitive to sediment
382 cohesion, while the shear vane measurement is probably more responsive to friction angle. By
383 employing multiple methods, each measuring sediment properties in slightly different ways, a
384 nuanced understanding of mechanisms by which vegetation affects sediment stability both directly
385 and indirectly is established. For example, sediment cohesion, or the emulation thereof by root
386 systems, emerges as the geotechnical attribute that appears most directly to relate to erodibility, as
387 would be measured by hydrodynamic exposure and subsequent observation of erosion. The field
388 shear vane data provide an indication that vegetation cover enhances shear strength. This emerges
389 from the contrasts between, for example WS PUC and WS BARE. The lack of contrast between TF
390 PUC and WS SAL/SPA where one exists between these WS cover types and the other TF cover types
391 also suggests that *Puccinellia*, in particular, increases shear vane measurements. There is a
392 consistent relative pattern of shear strengths by cover type at each site, with bare ground being
393 lowest and *Puccinellia* being highest. While these within-site differences are not statistically
394 significant given the power of the non-parametric tests that were appropriate to this dataset, this
395 consistency offers some indication that the differences in shear strength between cover types are
396 not random. The magnitude of any 'vegetation effect' appears to be larger in the coarser sediments
397 of WS, where *Puccinellia* emerges as statistically different from bare ground. This aligns with the
398 findings of, for example, De Battisti et al (2019). These observations do not, however, necessarily
399 imply that vegetation cover directly causes any differences in shear strength.

400 It has been argued that edaphic factors, rather than biotic ones, are the primary control of species
401 zonation within a saltmarsh (Adam, 1990). Notwithstanding that intra-specific variability in tolerance
402 or adaptation to these factors also exists, subsequent research has tended to confirm this assertion,
403 finding relationships between vegetation growth and substrate properties such as salinity (Snow &
404 Vince, 1984). Effects on inter-specific competition caused by waterlogging and sedimentology have
405 been observed (Huckle et al., 2000) while Cui et al.(2011) identified spatially variable relationships
406 between plant communities and edaphic factors such as bulk density, pH, salinity and moisture
407 content along a topographic gradient. De Battisti et al. (2019) find that *Spartina* root densities are
408 partially controlled by soil redox potential. Moffett and Gorelick (2016) also document spatial
409 associations between plant species type and soil geochemistry, although Chiról et al. (2021a) find no
410 intra-site variability in sodium absorption ratio related to species cover at the sites studied here.
411 Vegetation has been shown to exert reciprocal controls on soil properties such as drainage, organic
412 content and geochemistry, thus altering edaphic conditions (Caçador et al., 2000; Gebrehiwet et al.,
413 2008; Koretsky et al., 2008). More recently these studies have been extended to assess the role of
414 hydrodynamic exposure in determining survivorship of different species (Schoutens et al., 2021),
415 introducing an additional dimension of abiotic complexity. Thus, the distribution of vegetation within
416 the intertidal zone is closely coupled to many substrate parameters that are likely to influence shear
417 strength and erodibility.

418 It is likely, therefore, that the differences in shear strength that we observe reflect the combined
419 influence of these parameters alongside any mechanical modifications to the soil matrix arising from
420 the plant elements themselves. This raises the question of what the relative contributions of these
421 processes are to the substrate shear strength and, potentially more importantly, to sediment
422 erodibility. Analogues in other vegetated soil systems (e.g. O’loughlin & Ziemer, 1982) and the
423 emerging literature in the context of salt marshes (e.g. Chen et al., 2019; Ford et al., 2016; Gillen et
424 al., 2020), as well as the findings we present here, all provide evidence that vegetation does make a
425 significant contribution to soil shear strength through direct, mechanical means, but our results also
426 suggest potential indirect interactions with erosion processes. Thus, block failure resulting from low
427 bulk shear strength may increase the surface area of exposed sediment (Allen, 1989). Blocks, once
428 fallen to occupy lower surface elevations are also exposed to higher magnitude/frequency of
429 wave/tide forcing and thus greater likelihood of grain-by-grain erosion.

430 Our exploratory modelling using BRTs consistently selected the surface cover type on saltmarsh
431 substrates as being an important predictor of substrate shear strength. At WS, the contribution of
432 cover type was the dominant factor in a model that accounts for most of the variance in shear
433 strength across the site. At TF, model performance was poorer but cover type was the joint most
434 important predictor, alongside the percentage of sediment below 63 μm in size. The relative
435 patterns of the magnitude of influence of different surface cover types are consistent between sites.
436 This reinforces the conclusion that *Puccinellia* increases sediment shear strength most, while
437 unvegetated substrates tend to have the lowest shear strengths. This observation is further borne
438 out by the torvane measurements conducted in the laboratory, which suggest the same sequence of
439 relative shear strength effects within TF. The good performance of the BRT model at WS, where
440 training correlation was 0.90, and its strong dependence on cover type (38%), suggests that
441 vegetation presence and composition has a greater influence on shear strength in sandier sediments
442 than it does in clay-rich environments. Furthermore, it suggests that, at least for sandier
443 environments, the mapping of vegetation distributions could provide insight to a significant
444 component of the spatial variability in substrate shear strengths. The strong vegetation influence in
445 sandy systems, also identified as suppressing erosion rates measured in the field (Lo et al., 2017),
446 potentially arises because the root networks are able to reinforce the coarser sediment matrix in
447 ways that bind the sediments together to mitigate the lack of cohesion in such substrates. This may
448 be facilitated for different species in different ways through mechanical or geochemical
449 modification of the substrates, or through the introduction of root exudates and their effects on the
450 rhizosphere (e.g. Wang et al., 2016). Where clay content is higher, however, any such effect may be
451 less significant because cohesion is higher anyway. Observations of intra-specific differences in root
452 morphology between the two sedimentologies investigated here were observed at the same sites by
453 Chiról et al. (2021a); they attribute these to the relative ease of root penetration, and thus more
454 extensive network formation, in the sandier WS sediments compared to those of the TF site. A
455 similar phenomenon of more extensive root networks being observed in sandier sediments was also
456 discussed by De Battisti et al (2019) although alternative causes of differences in network
457 morphology and plant allometry have also been proposed, such as salinity (De Battisti et al., 2020) or
458 wave exposure (Cao et al., 2020), which may be independent of site sedimentology. Structural
459 differences in root network attributes may therefore account for some of the observed contrast in
460 cover type effect on geotechnical properties between sites (Figure 4, Figure 6).

461 The fact that percentage organic content was selected by the BRT models at both sites, albeit as the
462 least informative predictor, is instructive. This finding suggests that vegetation effects over longer
463 timescales are also important. Broadly speaking, higher organic matter contents were associated
464 with higher shear strengths at a within-site scale (Figure 7). Autochthonous organic matter

465 accumulation arises from the primary productivity of the vegetation cover and its subsequent
466 decomposition. Sediment organic matter content therefore reflects, in part, the vegetation history
467 of the location, notwithstanding that organic material may be imported or exported (Alongi, 2020;
468 Ganju et al., 2019). As such, a relatively small component of sediment shear strength at both sites
469 appears to be dependent on longer-term vegetation attributes which may or may not be reflected in
470 the present-day species distributions. The magnitude of this effect and the timescales over which it
471 develops and operates are a topic for further study.

472 The laboratory-based geotechnical tests allowed for the further exploration as to how vegetation
473 alters sediment shear strength. The shear box data only showed a significant difference for the
474 cohesion values of WS BARE and TF PUC, with the higher cohesion in TF PUC probably being related
475 to a combination of sedimentological differences (higher clay content) and the effect of the
476 *Puccinellia* root system. The pattern of relative parameter values was, however, consistent with
477 other measurements, such as the shear vane, and can be explained by existing mechanistic
478 understandings. It is possible, therefore, that the results may hint at findings that may become
479 significant with additional data. Whilst it is not possible to draw robust statistical inferences from
480 this dataset, the pattern of differences between cover types does suggest that vegetation presence
481 and species may alter the properties of the underlying sediments. The position of WS BARE as having
482 the highest friction angle and lowest cohesion was consistent with what would be expected based
483 on the sedimentology of the two sites. TF BARE and TF PUC both have low friction angles, while that
484 for TF SPA is almost the same as WS BARE, despite the sediment matrix being composed of much
485 finer particles. It would appear that the *Spartina* root system (De Battisti et al., 2019) may interact
486 with the sediments in a way that emulates a coarser particle size distribution and therefore a higher
487 friction angle where bulk failure processes are concerned. In contrast, the TF BARE and TF SPA
488 cohesion values were very similar, while that for TF PUC was much higher. The *Spartina* root system
489 therefore does not appear to have much effect on the bulk sediment behaviour related to cohesive
490 strength, while *Puccinellia* may act to increase apparent cohesion.

491 It is important to note that these geotechnical tests are typically conducted and interpreted in the
492 context of sediments that do not contain plant elements. The friction angle therefore usually refers
493 to the angle through which a grain of sediment must be raised in order to lift the material free of the
494 matrix and allow shear to take place. Thus, cohesion typically refers to the strength of the sediment
495 at no normal load, a function of the electrostatic forces between particles. Plant root networks have
496 long been considered to contribute primarily to the cohesion component in the context of hillslope
497 processes (e.g. O'loughlin & Ziemer, 1982), although our observations here suggest that *Spartina*
498 roots may result in elevated friction angles while having minimal influence on cohesion (Figure 4). It
499 is unlikely that the differences that were observed in these test parameters in the presence of plant
500 root networks arise from the same differences in physical processes and forces that could be
501 inferred for 'pure' sediments. If the inter-particle interactions controlling the measured friction angle
502 and cohesion values are similar between samples from a given site, then the mechanical root
503 network effect is acting to *emulate* a modification of these parameters. Future work focusing on
504 understanding the physics of this emulation would be a valuable contribution towards characterising
505 biosedimentary system behaviours. The results observed in this study make intuitive sense when
506 considering the behaviour of the differing root morphologies in the context of planar shear, as
507 imposed by the shear box apparatus. The large, vertical tap-root system of *Spartina* (visible as round
508 features representing root cross-sections viewed from above in Figure 3) is relatively rigid and
509 unlikely to be sheared or bent within the shear box test. To allow strain within the matrix
510 surrounding them, the strong vertical root segments would need to be rotated towards the
511 horizontal plane during shearing, displacing sediment while doing so. By contrast, small, fibrous

512 *Puccinellia* roots, however, are likely to merely bend along the shear plane until they come into
513 tension; their tensile strength thereafter may account for the apparently elevated cohesion
514 measurements. It is therefore hypothesised that different plant species may modify the bulk
515 responses of sediments to shear forces in ways that appear as altered friction angles or cohesion
516 values. The physics of the distribution of forces within the sediment, however, will be different to
517 those normally inferred from measured friction angles / cohesion. In terms of predicting the
518 response to erosive forces in a field situation, this distinction may become important, and the
519 importance of the root-induced geotechnical differences will vary depending on the mode of failure
520 being considered. For example, the *Puccinellia* root system may increase resistance to the formation
521 of tension cracks and toppling failures, while the vertical *Spartina* roots may provide more resistance
522 to rotational slumping. Again, further research is required if the function of these root systems in
523 controlling various modes of erosion is to be understood.

524 The triaxial test results showed that simulating realistic conditions with small overburdens is
525 challenging, both in terms of the precision of the equipment deployed and the behaviours of the
526 sediments being tested. A few studies exist, however, that have used triaxial tests to assess the
527 contribution of root elements to sediment properties. For example, Patel and Singh (2020) found
528 small increases in shear strength measured by triaxial test conferred to artificial mixtures of clayey
529 and sandy sediments containing glass fibre reinforcement. Meng et al. (2020) also observed
530 variability in shear strength related to the rooting geometry of Golden Vicary Privet (*Ligustrum spp.*)
531 in a controlled planting experiment and found that the root network's effect was largely to enhance
532 the sediment cohesion rather than friction angle. As noted previously in the context of the shear
533 box, this is unlikely to represent a true increase in cohesion but rather soil-root interactions
534 presenting a similar phenomenon within the context of the parameters measured by the test. It
535 seems likely that triaxial testing could furnish valuable insights to the role of vegetation elements in
536 determining salt marsh stability, but, given the nature of the sediments and conditions that need to
537 be simulated, this may prove challenging. It is important to note that the different storage durations
538 for each sample may contribute to the patterns observed in the laboratory geotechnical tests.

539 The bulk density measurements suggest that, irrespective of site sedimentology, unvegetated
540 sediments have higher bulk densities than their vegetated counterparts. *Spartina* seems to be
541 associated with the lowest bulk densities at both sites. All else being equal, higher bulk density tends
542 to reduce erodibility (Watts et al., 2003; Winterwerp et al., 2012). The data presented here suggest
543 that the presence of vegetation decouples the expected relationship between bulk density and
544 sediment stability, in that vegetated sites with lower bulk densities than bare sites nevertheless
545 consistently exhibit higher shear strength, friction angle and cohesion, irrespective of the method
546 used to measure these attributes. The presence of vegetation therefore confers strength to the
547 sediment greater than that which may be lost by the attendant reduction in bulk density. Within the
548 vegetated cover types for each site, the relative pattern of bulk density tends to reflect the relative
549 pattern of, for example, shear strength. This suggests that changes in bulk density may represent an
550 indirect mechanism whereby vegetation type interacts with substrate geotechnical properties.

551 The findings of this study provide the basis for conceptual models of how various vegetation
552 distributions, perhaps related to site topography, might result in spatio-temporal variations in
553 vulnerability to erosion. This concept is here explored through the example of the erosional setting
554 of the TF site. The saltmarsh – mudflat margin at TF is ramped, rather than cliffed, with a shore-
555 normal ridge-runnel morphology superimposed on the general seaward slope. Erosion therefore
556 manifests itself as the retreat of a relatively wide zone of elevation loss over a relatively shallow
557 slope. Removal of material at the transition from marsh to mudflat may lead to lowered sediment

558 surface elevations, increased hydroperiod and a transition to a vegetation community dominated by
559 pioneer species (Adam, 1990; Feagin et al., 2010; Moody et al., 2013). Given the erosional setting,
560 the pioneer-dominated seaward fringe presumably represents the previous location of a higher
561 marsh platform dominated by *Puccinellia* and *Atriplex*, as is still observed to landward. We show that
562 the pioneer species are associated with lower shear strengths and cohesion than *Puccinellia*.
563 Whether sediment shear strength or cohesion, as measured by the techniques described above is
564 the best proxy for the substrate's ability to resist erosion remains, to some extent, an open question.
565 If, however, higher shear strengths or increased cohesion imply reduced erodibility for a given
566 hydrodynamic exposure, then the vulnerability of the seaward zone of the marsh may increase
567 following a transition from mature to pioneer vegetation, supplying a positive feedback that
568 accelerates retreat rates. Our study suggests that within-site variations in geotechnical properties
569 likely result from a combination of factors, including vegetation species transitions and organic
570 matter contents. Over time, changes in the saltmarsh community, including those enforced through
571 direct (e.g., grazing) or indirect (e.g., sea level rise) interventions, may thus act to influence the rate
572 at which marsh margins can erode. Conceptualising the linkage between marsh to tidal flat transition
573 morphology, sedimentology, and vegetation in this way provides a potential mechanism by which
574 margin morphology is linked to erosion rates, as suggested by other studies (Evans et al., 2019;
575 Finotello et al., 2020; Tonelli et al., 2010). Further insights into these interactions are now needed,
576 not least in light of evidence of the positive elevational response of saltmarsh surfaces under
577 *Puccinellia* to enhanced CO₂ (Reef et al., 2016) and of low surficial erosion under *Puccinellia* in
578 extreme storm surge conditions (Spencer et al., 2016). Emphasis must be placed on the
579 understanding of interactions between vegetation, root morphology and soil geochemistry in future
580 studies in order to address these specific species-level controls on saltmarsh landform evolution.

581

582 **Conclusions:**

583 Salt marsh vegetation distributions are responsive to edaphic and other factors relating to site
584 topology while at the same time engineering these factors via biophysical feedbacks. Disentangling
585 which factors dominate the spatial variability in substrate shear strength remains a challenging
586 problem. Nevertheless, vegetation distributions and types show associations with variability of
587 sediment geotechnical parameters within sites. To what extent vegetation is responsive to, or
588 determinative of, that variability in properties may be of secondary importance for applied
589 purposes. Different halophyte species also affect components of the shear strength, such as
590 cohesion and friction angle, in different ways that appear to relate to root morphology. We
591 therefore conclude that the mechanical deformation of root networks under shear, which involves
592 different force vectors depending on root morphology, contributes substantially to the observed
593 variability in shear strength. Vegetation mapping may therefore provide useful insight to the spatial
594 variability of substrate geotechnical properties. The direct effects of root networks on cohesion and
595 friction angle, however, are unlikely to reflect true modifications of these parameters as they would
596 be interpreted in root-free sediments. The secondary effects of roots on soil structure and
597 geochemistry probably affect its mechanical properties such as cohesion in a stricter sense and may
598 be more important in terms of determining marsh substrate vulnerability to particulate scale erosion
599 than those conferred mechanically. We argue that, while useful, shear strength alone is an
600 inadequate descriptor of erodibility for the purposes of predicting rates of morphological change.
601 Components of sediment strength such as cohesion emerge from this study as more closely
602 representing the expected erodibility of sediments under hydrodynamic forcing. This aspect will be
603 explored further in future work. A more nuanced conversation, one that is explicit about the time

604 and space scales of interest and addresses appropriate erosion processes, controls and measures of
605 erodibility, is required in order to advance our understanding, and representation, of marsh
606 erosional processes beyond simplistic assumptions about relationships between shear strength and
607 morphological change. In order to better constrain the processes through which vegetation affects
608 erodibility, and on what timescales, will require further detailed experimental investigation using
609 multiple methods, controlling for multiple factors, and exposing sediments to realistic erosive forces.
610 This, coupled with a body of literature on the effects of cumulative, longer-term hydrodynamic
611 forcing, will facilitate the morphodynamic predictions required to support effective coastal
612 management.

613

614 [References:](#)

- 615 Adam, P. (1990). *Saltmarsh Ecology*. Cambridge, UK: Cambridge University Press.
- 616 Ali, F. H., & Osman, N. (2008). Shear Strength of a Soil Containing Vegetation Roots. *Soils and*
617 *Foundations*, 48(4), 587–596. <https://doi.org/10.3208/SANDF.48.587>
- 618 Allen, J. R. L. (1989). Evolution of salt-marsh cliffs in muddy and sandy systems: A qualitative
619 comparison of British West-Coast estuaries. *Earth Surface Processes and Landforms*, 14(1), 85–
620 92. <https://doi.org/10.1002/esp.3290140108>
- 621 Alongi, D. M. (2020). Carbon Balance in Salt Marsh and Mangrove Ecosystems: A Global Synthesis.
622 *Journal of Marine Science and Engineering*, 8(10), 767. <https://doi.org/10.3390/jmse8100767>
- 623 De Battisti, D., Fowler, M. S., Jenkins, S. R., Skov, M. W., Rossi, M., Bouma, T. J., et al. (2019).
624 Intraspecific Root Trait Variability Along Environmental Gradients Affects Salt Marsh Resistance
625 to Lateral Erosion. *Frontiers in Ecology and Evolution*, 7(May), 1–11.
626 <https://doi.org/10.3389/fevo.2019.00150>
- 627 De Battisti, D., Fowler, M. S., Jenkins, S. R., Skov, M. W., Bouma, T. J., Neyland, P. J., & Griffin, J. N.
628 (2020). Multiple trait dimensions mediate stress gradient effects on plant biomass allocation,
629 with implications for coastal ecosystem services. *Journal of Ecology*, 108(4), 1227–1240.
630 <https://doi.org/10.1111/1365-2745.13393>
- 631 Bernik, B., Pardue, J., & Blum, M. (2018). Soil erodibility differs according to heritable trait variation
632 and nutrient-induced plasticity in the salt marsh engineer *Spartina alterniflora*. *Marine Ecology*
633 *Progress Series*, 601, 1–14. <https://doi.org/10.3354/meps12689>
- 634 Brooks, H., Möller, I., Carr, S., Chirol, C., Christie, E., Evans, B., et al. (2021). Resistance of salt marsh
635 substrates to near-instantaneous hydrodynamic forcing. *Earth Surface Processes and*
636 *Landforms*, 46(1), 67–88. <https://doi.org/10.1002/esp.4912>
- 637 Caçador, M. I., Madureira, M. J., & Vale, C. (2000). Effects of plant roots on salt-marsh sediment
638 geochemistry. *Proceedings in Marine Science*, 2(C), 197–204. [https://doi.org/10.1016/S1568-2692\(00\)80016-9](https://doi.org/10.1016/S1568-2692(00)80016-9)
- 640 Cao, H., Zhu, Z., James, R., Herman, P. M. J., Zhang, L., Yuan, L., & Bouma, T. J. (2020). Wave effects
641 on seedling establishment of three pioneer marsh species: survival, morphology and
642 biomechanics. *Annals of Botany*, 125(2), 345–352. <https://doi.org/10.1093/aob/mcz136>
- 643 Chen, Y., Thompson, C., & Collins, M. (2019). Controls on creek margin stability by the root systems
644 of saltmarsh vegetation, Beaulieu Estuary, Southern England. *Anthropocene Coasts*, 2(1), 21–
645 38. <https://doi.org/10.1139/anc-2018-0005>
- 646 Chirol, C., Spencer, K. L., Carr, S. J., Möller, I., Evans, B., Lynch, J., et al. (2021). Effect of vegetation

- 647 cover and sediment type on 3D subsurface structure and shear strength in saltmarshes. *Earth*
648 *Surface Processes and Landforms*, 46(11), 2279–2297. <https://doi.org/10.1002/esp.5174>
- 649 Chiroi, C., Carr, S. J., Spencer, K. L., & Moeller, I. (2021). Pore, live root and necromass quantification
650 in complex heterogeneous wetland soils using X-ray computed tomography. *Geoderma*, 387,
651 114898. <https://doi.org/10.1016/j.geoderma.2020.114898>
- 652 Chmura, G. L. (2013). What do we need to assess the sustainability of the tidal salt marsh carbon
653 sink? *Ocean & Coastal Management*, 83, 25–31.
654 <https://doi.org/10.1016/j.ocecoaman.2011.09.006>
- 655 Crosby, S. C., Sax, D. F., Palmer, M. E., Booth, H. S., Deegan, L. A., Bertness, M. D., & Leslie, H. M.
656 (2016). Salt marsh persistence is threatened by predicted sea-level rise. *Estuarine, Coastal and*
657 *Shelf Science*, 181, 93–99. <https://doi.org/10.1016/j.ecss.2016.08.018>
- 658 Cui, B. S., He, Q., & An, Y. (2011). Community Structure and Abiotic Determinants of Salt Marsh Plant
659 Zonation Vary Across Topographic Gradients. *Estuaries and Coasts*, 34(3), 459–469.
660 <https://doi.org/10.1007/s12237-010-9364-4>
- 661 Elith, J., Leathwick, J. R., & Hastie, T. (2008). A working guide to boosted regression trees. *Journal of*
662 *Animal Ecology*, 77(4), 802–813. <https://doi.org/10.1111/j.1365-2656.2008.01390.x>
- 663 Evans, B. R., Möller, I., Spencer, T., & Smith, G. (2019). Dynamics of salt marsh margins are related to
664 their three-dimensional functional form. *Earth Surface Processes and Landforms*, 44(9), 1816–
665 1827. <https://doi.org/10.1002/esp.4614>
- 666 Feagin, R. A. , Martinez, M. L. , Mendoza-Gonzalez, G. , & Costanza, R. . (2010). Salt marsh zonal
667 migration and ecosystem service change in response to global sea level rise: A case study from
668 an urban region. *Ecology and Society*, 15(4), Art. 14 (online).
- 669 Finotello, A., Marani, M., Carniello, L., Pivato, M., Roner, M., Tommasini, L., & D'alpaos, A. (2020).
670 Control of wind-wave power on morphological shape of salt marsh margins. *Water Science and*
671 *Engineering*, 13(1), 45–56. <https://doi.org/10.1016/j.wse.2020.03.006>
- 672 Ford, H., Garbutt, A., Ladd, C., Malarkey, J., & Skov, M. W. (2016). Soil stabilization linked to plant
673 diversity and environmental context in coastal wetlands. *Journal of Vegetation Science*, 27(2),
674 259–268. <https://doi.org/10.1111/jvs.12367>
- 675 Friess, D. a, Krauss, K. W., Horstman, E. M., Balke, T., Bouma, T. J., Galli, D., & Webb, E. L. (2012). Are
676 all intertidal wetlands naturally created equal? Bottlenecks, thresholds and knowledge gaps to
677 mangrove and saltmarsh ecosystems. *Biological Reviews of the Cambridge Philosophical*
678 *Society*, 87(2), 346–66. <https://doi.org/10.1111/j.1469-185X.2011.00198.x>
- 679 Ganju, N. K., Defne, Z., Elsey-Quirk, T., & Moriarty, J. M. (2019). Role of Tidal Wetland Stability in
680 Lateral Fluxes of Particulate Organic Matter and Carbon. *Journal of Geophysical Research:*
681 *Biogeosciences*, 124(5), 1265–1277. <https://doi.org/10.1029/2018JG004920>
- 682 Gebrehiwet, T., Koretsky, C. M., & Krishnamurthy, R. V. (2008). Influence of *Spartina* and *Juncus* on
683 saltmarsh sediments. III. Organic geochemistry. *Chemical Geology*, 255(1–2), 114–119.
684 <https://doi.org/10.1016/j.chemgeo.2008.06.015>
- 685 Gillen, M., Messerschmidt, T., & Kirwan, M. (2020). Biophysical controls of marsh soil shear strength
686 along an estuarine salinity gradient. *Earth Surface Dynamics Discussions*, 1–15.
687 <https://doi.org/10.5194/esurf-2020-58>
- 688 Grabowski, R. C., Droppo, I. G., & Wharton, G. (2011). Erodibility of cohesive sediment: The
689 importance of sediment properties. *Earth-Science Reviews*, 105(3–4), 101–120.

690 <https://doi.org/10.1016/J.EARSCIREV.2011.01.008>

691 Huckle, J. M., Potter, J. A., & Marrs, R. H. (2000). Influence of environmental factors on the growth
692 and interactions between salt marsh plants: Effects of salinity, sediment and waterlogging.
693 *Journal of Ecology*, 88(3), 492–505. <https://doi.org/10.1046/j.1365-2745.2000.00464.x>

694 Jafari, N. H., Harris, B. D., Cadigan, J. A., Day, J. W., Sasser, C. E., Kemp, G. P., et al. (2019). Wetland
695 shear strength with emphasis on the impact of nutrients, sediments, and sea level rise.
696 *Estuarine, Coastal and Shelf Science*, 229, 106394. <https://doi.org/10.1016/j.ecss.2019.106394>

697 Koretsky, C. M., Haveman, M., Cuellar, A., Beuving, L., Shattuck, T., & Wagner, M. (2008). Influence
698 of *Spartina* and *Juncus* on Saltmarsh Sediments. I. Pore Water Geochemistry. *Chemical*
699 *Geology*, 255(1–2), 87–99. <https://doi.org/10.1016/j.chemgeo.2008.06.013>

700 Leonardi, N., Ganju, N. K., & Fagherazzi, S. (2016). A linear relationship between wave power and
701 erosion determines salt-marsh resilience to violent storms and hurricanes. *Proceedings of the*
702 *National Academy of Sciences*, 113(1), 64–68. <https://doi.org/10.1073/pnas.1510095112>

703 Lo, V. B. B., Bouma, T. J. J., van Belzen, J., Van Colen, C., & Airoldi, L. (2017). Interactive effects of
704 vegetation and sediment properties on erosion of salt marshes in the Northern Adriatic Sea.
705 *Marine Environmental Research*, 131, 32–42. <https://doi.org/10.1016/j.marenvres.2017.09.006>

706 Marin-Diaz, B., Govers, L. L., Wal, D., Olff, H., & Bouma, T. J. (2021). How grazing management can
707 maximize erosion resistance of salt marshes. *Journal of Applied Ecology*, 58(7), 1533–1544.
708 <https://doi.org/10.1111/1365-2664.13888>

709 McOwen, C., Weatherdon, L., Bochove, J.-W., Sullivan, E., Blyth, S., Zockler, C., et al. (2017). A global
710 map of saltmarshes. *Biodiversity Data Journal*, 5, e11764.
711 <https://doi.org/10.3897/BDJ.5.e11764>

712 Meng, S., Zhao, G., & Yang, Y. (2020). Impact of Plant Root Morphology on Rooted-Soil Shear
713 Resistance Using Triaxial Testing. *Advances in Civil Engineering*, 2020, Art ID8825828 (online),
714 13 pages. <https://doi.org/10.1155/2020/8825828>

715 Miller, A. (2002). *Subset selection in regression* (1st ed.). Boca Raton: Chapman & Hall/CRC.

716 Moffett, K. B., & Gorelick, S. M. (2016). Relating salt marsh pore water geochemistry patterns to
717 vegetation zones and hydrologic influences. *Water Resources Research*, 52(3), 1729–1745.
718 <https://doi.org/10.1002/2015WR017406>

719 Möller, I., Kudella, M., Rupprecht, F., Spencer, T., Paul, M., van Wesenbeeck, B. K., et al. (2014).
720 Wave attenuation over coastal salt marshes under storm surge conditions. *Nature Geoscience*,
721 7(10), 727–731. <https://doi.org/10.1038/ngeo2251>

722 Moody, R., Cebrian, J., Kerner, S., Heck, K., Powers, S., & Ferraro, C. (2013). Effects of shoreline
723 erosion on salt-marsh floral zonation. *Marine Ecology Progress Series*, 488, 145–155.
724 <https://doi.org/10.3354/meps10404>

725 Mouazen, A. M. (2002). Mechanical behaviour of the upper layers of a sandy loam soil under shear
726 loading. *Journal of Terramechanics*, 39(3), 115–126. [https://doi.org/10.1016/S0022-](https://doi.org/10.1016/S0022-4898(02)00008-3)
727 [4898\(02\)00008-3](https://doi.org/10.1016/S0022-4898(02)00008-3)

728 ntslf.org. (2021). National Tide and Sea Level Facility. Retrieved 7 June 2021, from ntslf.org

729 O’loughlin, C., & Ziemer, R. R. (1982). *The importance of root strength and deterioration rates upon*
730 *edaphic stability in steepland forests. Proceedings of I.U.F.R.O. Workshop P.1.07-00 Ecology of*
731 *Subalpine Ecosystems as a Key to Management. 2-3 August 1982, Corvallis, Oregon. Oregon*
732 *State University, Corvallis, Oregon. p. 70-78.*

733 Patel, S. K., & Singh, B. (2020). A Comparative Study on Shear Strength and Deformation Behaviour
734 of Clayey and Sandy Soils Reinforced with Glass Fibre. *Geotechnical and Geological Engineering*,
735 38(5), 4831–4845. <https://doi.org/10.1007/s10706-020-01330-5>

736 R Core Team. (2013). R: A Language and Environment for Statistical Computing. Vienna, Austria.

737 Reef, R., Spencer, T., Möller, I., Lovelock, C. E., Christie, E. K., Mcivor, A. L., et al. (2016). The effects
738 of elevated CO₂ and eutrophication on surface elevation gain in a European salt marsh. *Global*
739 *Change Biology*. <https://doi.org/10.1111/gcb.13396>

740 Schoutens, K., Reents, S., Nolte, S., Evans, B., Paul, M., Kudella, M., et al. (2021). Survival of the
741 thickest? Impacts of extreme wave-forcing on marsh seedlings are mediated by species
742 morphology. *Limnology and Oceanography*, Ino.11850. <https://doi.org/10.1002/lno.11850>

743 Snow, A. A., & Vince, S. W. (1984). Plant Zonation in an Alaskan Salt Marsh: II. An Experimental Study
744 of the Role of Edaphic Conditions. *The Journal of Ecology*, 72(2), 669–684.
745 <https://doi.org/10.2307/2260075>

746 Spencer, T., Möller, I., Rupprecht, F., Bouma, T. J., van Wesenbeeck, B. K., Kudella, M., et al. (2016).
747 Salt marsh surface survives true-to-scale simulated storm surges. *Earth Surface Processes and*
748 *Landforms*, 41(4). <https://doi.org/10.1002/esp.3867>

749 Tolhurst, T. J., Riethmüller, R., & Paterson, D. M. (2000). In situ versus laboratory analysis of
750 sediment stability from intertidal mudflats. *Continental Shelf Research*, 20(10–11), 1317–1334.
751 [https://doi.org/10.1016/S0278-4343\(00\)00025-X](https://doi.org/10.1016/S0278-4343(00)00025-X)

752 Tonelli, M., Fagherazzi, S., & Petti, M. (2010). Modeling wave impact on salt marsh boundaries.
753 *Journal of Geophysical Research*, 115(C9), C09028. <https://doi.org/10.1029/2009JC006026>

754 Wang, H., van der Wal, D., Li, X., van Belzen, J., Herman, P. M. J., Hu, Z., et al. (2017). Zooming in and
755 out: Scale dependence of extrinsic and intrinsic factors affecting salt marsh erosion. *Journal of*
756 *Geophysical Research: Earth Surface*, 122(7), 1455–1470.
757 <https://doi.org/10.1002/2016JF004193>

758 Wang, J.-J., Zhang, H.-P., Tang, ; Sheng-Chuan, & Liang, Y. (2013). Effects of Particle Size Distribution
759 on Shear Strength of Accumulation Soil. *Journal of Geotechnical and Geoenvironmental*
760 *Engineering*, 139(11), 1994–1997. [https://doi.org/10.1061/\(ASCE\)GT.1943-5606.0000931](https://doi.org/10.1061/(ASCE)GT.1943-5606.0000931)

761 Wang, M., Yang, P., & Falcão Salles, J. (2016). Distribution of Root-Associated Bacterial Communities
762 Along a Salt-Marsh Primary Succession. *Frontiers in Plant Science*, 6, Art. 1188 (online) 11
763 pages. <https://doi.org/10.3389/fpls.2015.01188>

764 Watts, C. W., Tolhurst, T. J., Black, K. S., & Whitmore, A. P. (2003). In situ measurements of erosion
765 shear stress and geotechnical shear strength of the intertidal sediments of the experimental
766 managed realignment scheme at Tollesbury, Essex, UK. *Estuarine, Coastal and Shelf Science*,
767 58(3), 611–620. [https://doi.org/10.1016/S0272-7714\(03\)00139-2](https://doi.org/10.1016/S0272-7714(03)00139-2)

768 Winterwerp, J. C., van Kesteren, W. G. M., van Prooijen, B., & Jacobs, W. (2012). A conceptual
769 framework for shear flow–induced erosion of soft cohesive sediment beds. *Journal of*
770 *Geophysical Research: Oceans*, 117(C10), 1–17. <https://doi.org/10.1029/2012JC008072>

771 Zhou, G. G. D., Chen, L. lei, Mu, Q. yi, Cui, K. F. E., & Song, D. ri. (2019). Effects of water content on
772 the shear behavior and critical state of glacial till in Tianmo Gully of Tibet, China. *Journal of*
773 *Mountain Science* 2019 16:8, 16(8), 1743–1759. <https://doi.org/10.1007/S11629-019-5440-9>

774

775 Acknowledgements

776 We would like to acknowledge the input of Simon Carr, Lee Jones, Olivia Shears, Elizabeth Christie,
777 Andrew Cliff and Keith Ord to this work, alongside the support of the landowners of the sites used.
778 This work was funded by UKRI Natural Environment Research Council (NERC) grant RESIST-UK (grant
779 number NE/R01082X/1). Further support was provided by the University of Cambridge in the form of
780 additional funds to address COVID-19-related delays. The work described in this publication was
781 supported by the European Community's Horizon 2020 Research and Innovation Programme
782 through the grant to HYDRALA=PLUS, Contract no. 654110 and is a contribution to UKRI NERC
783 "Physical and Biological dynamic coastal processes and their role in coastal recovery" (BLUE-coast),
784 Grant Award Number: NE/NO015878/1. Further support was provided by NERC PhD Student-ship
785 (NE/L002507/1; 2016-2020), a Collaborative Award in Science and Engineering with the British
786 Geological Survey University Funding Initiative (BUFI) PhD studentship (S352 and the University of
787 Cambridge in the form of additional funds to address COVID-19-related delays. This paper is
788 published with permission of the Executive Director of the British Geological Survey.